ACS central science

Large Hyperpolarizabilities at Telecommunication-Relevant Wavelengths in Donor−Acceptor−Donor Nonlinear Optical Chromophores

Animesh Nayak,[†,‡] Jaehong Park,[†,‡] Kurt De Mey,[§] Xiangqian Hu,[†] Timothy V. Duncan,[‡] David N. Beratan,*[†,∥,⊥] Koen Clays,*[§] and Michael J. Therien*[†]

[†]Department of Chemistry, Duke University, French Family Science Center, 124 Science Drive, Durham, North Carolina 27708-0346, United States
[‡]Department of Chemistry, University of Pennsylvania, 231 South 34th Street, Philadelphia, Pennsylvania 19104-6323, United States
[§]Department of Chemistry, University of Leuven, B-3001 Leuven, Belgium
[∥]Department of Biochemistry, Duke University, Durham, North Carolina 27710, United States
[⊥]Department of Physics, Duke University, Durham, North Carolina 27708-0346, United States

Ⓢ *Supporting Information*

ABSTRACT: Octopolar D_2-symmetric chromophores, based on the MPZnM supermolecular motif in which (porphinato)-zinc(II) (PZn) and ruthenium(II) polypyridyl (M) structural units are connected via ethyne linkages, were synthesized. These structures take advantage of electron-rich *meso*-arylporphyrin or electron-poor *meso*-(perfluoroalkyl)porphyrin macrocycles, unsubstituted terpyridyl and 4′-pyrrolidinyl-2,2′;6′,2″-terpyridyl ligands, and modulation of metal(II) polypyridyl-to-(porphinato)zinc connectivity, to probe how

Hyperpolarizability (β_{HRS}) at 1500 nm = 4600 ± 1200 x 10⁻³⁰ esu

D_2 octopolar chromophore

electronic and geometric factors impact the measured hyperpolarizability. Transient absorption spectra obtained at early time delays ($t_{delay} < 400$ fs) demonstrate fast excited-state relaxation, and formation of a highly polarized T_1 excited state; the T_1 states of these chromophores display expansive, intense $T_1 \rightarrow T_n$ absorption manifolds that dominate the 800−1200 nm region of the NIR, long (μs) triplet-state lifetimes, and unusually large NIR excited absorptive extinction coefficients [$\varepsilon(T_1 \rightarrow T_n) \sim 10^5$ M⁻¹ cm⁻¹]. Dynamic hyperpolarizability (β_λ) values were determined from hyper-Rayleigh light scattering (HRS) measurements, carried out at multiple incident irradiation wavelengths spanning the 800−1500 nm spectral domain. The measured β_{HRS} value (4600 ± 1200 × 10⁻³⁰ esu) for one of these complexes, RuPZnRu, is the largest yet reported for any chromophore at a 1500 nm irradiation wavelength, highlighting that appropriate engineering of strong electronic coupling between multiple charge-transfer oscillators provides a critical design strategy to realize octopolar NLO chromophores exhibiting large β_{HRS} values at telecom-relevant wavelengths. Generalized Thomas−Kuhn sum (TKS) rules were utilized to compute the effective excited-state-to-excited-state transition dipole moments from experimental linear-absorption spectra; these data were then utilized to compute hyperpolarizabilities as a function of frequency, that include two- and three-state contributions for both β_{zzz} and β_{xzx} tensor components to the RuPZnRu hyperpolarizability spectrum. This analysis predicts that the β_{zzz} and β_{xzx} tensor contributions to the RuPZnRu hyperpolarizability spectrum maximize near 1550 nm, in agreement with experimental data. The TKS analysis suggests that relative to analogous dipolar chromophores, octopolar supermolecules will be likely characterized by more intricate dependences of the measured hyperpolarizability upon irradiation wavelength due to the interactions among multiple different β tensor components.
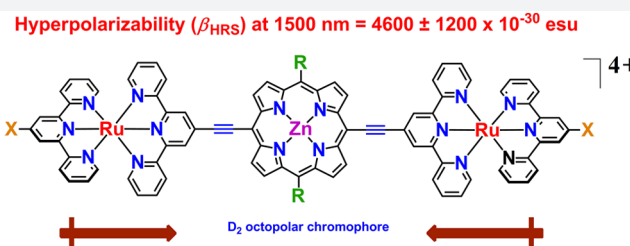
INTRODUCTION

Applications in telecommunications, data storage, sensor protection, and imaging drive interest in nonlinear optical (NLO) materials.[1−4] Organic NLO materials have been the focus of much attention due to their ease of processing, and the fact that molecular design can tailor the NLO responses for targeted applications.[2]

Dipolar chromophores based on a donor−bridge−acceptor (D-Br-A) framework define the most widely studied NLO motif.[5−20] The highly polarizable porphyrin unit figures prominently in many D-Br-A chromophores that exhibit large dynamic hyperpolarizabilities.[9,10,15,16,18−30] Earlier studies demonstrate that ethynyl linkages between multiple porphyrinic components, or between porphyrin moieties and other strong oscillators, give rise to unusually polarizable and hyperpolarizable chromophores[31−40] that manifest exciting NLO properties.[41−50]

Scheme 1. General Synthetic Scheme for Compounds 1–4[a,b]
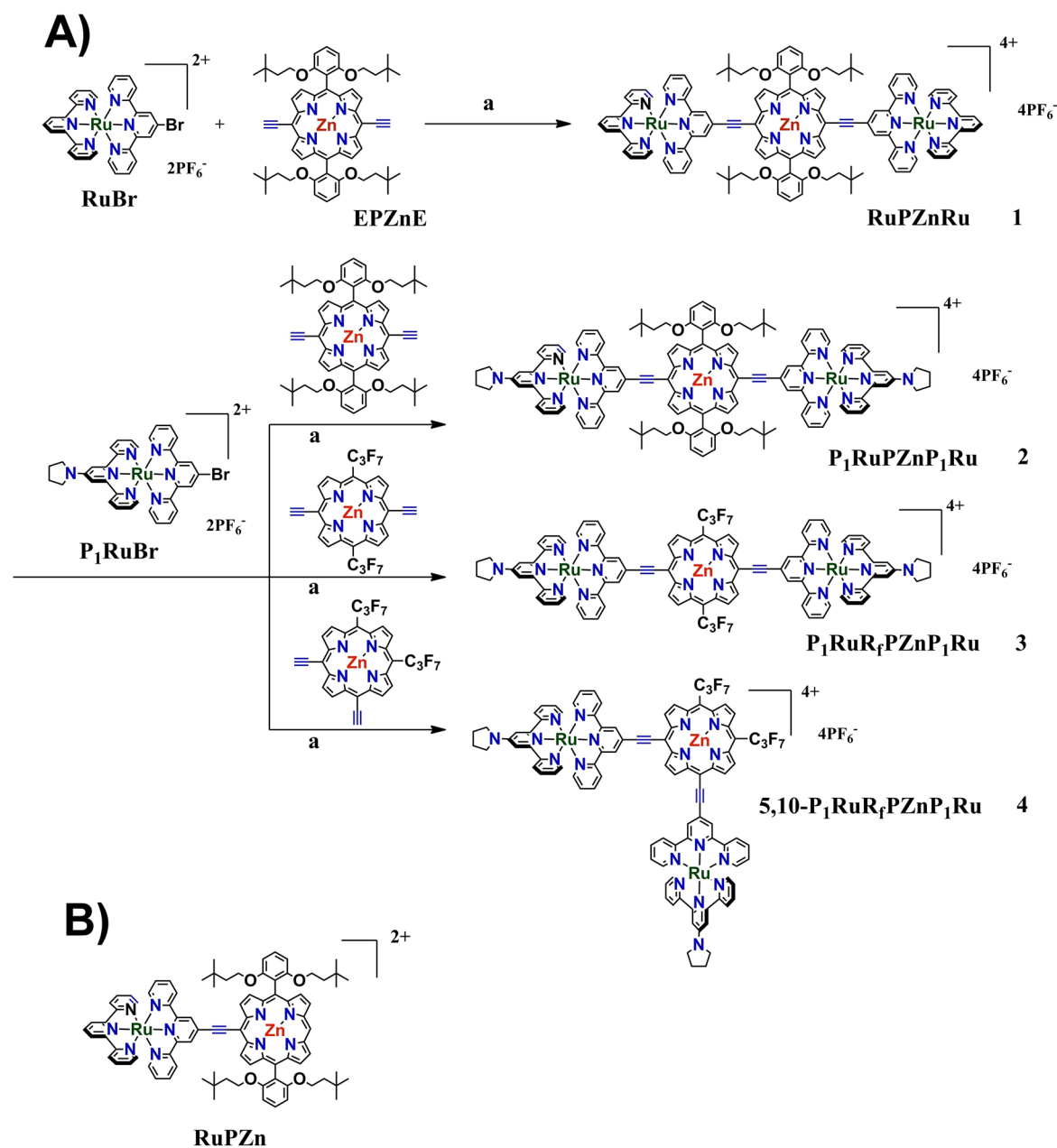
[a](A) Synthetic route to compounds **1–4**. (B) Molecular structure of **RuPZn**. [b](a) Pd$_2$(dba)$_3$, AsPh$_3$, THF, CH$_3$CN, Et$_3$N, 60 °C.

An interesting class of porphyrin-based chromophores are those in which (porphinato)zinc(II) (PZn) and metal(II) polypyridyl (M) units are linked via an ethyne bridge; many of these compositions feature extraordinarily large frequency-dependent first hyperpolarizabilities (i.e., high β_λ values). In these MPZn supermolecules, PZn π–π^* and (polypyridyl)-metal based charge-resonance absorption oscillator strength are extensively mixed, and the respective charge transfer (CT) transition dipoles of these chromophoric units are aligned along the highly conjugated molecular axis. These chromophores evince significant PZn–(polypyridyl)metal electronic interactions, display unusual dependences of the sign and magnitude of the hyperpolarizability upon the incident irradiation frequency, and exhibit substantial β_λ values at telecommunications-relevant wavelengths.[16,21–23,26,41,42,47]

Extensive research over the last several decades has led to the development of dipolar, D-Br-A chromophores having large hyperpolarizabilities across the 1300–1500 nm spectral domain.[6,12,16,51,52] Translation of large dipolar molecular hyperpolarizabilities into corresponding bulk-phase macro-scopic NLO materials requires ordering of the hyperpolarizable chromophores in a noncentrosymmetric fashion. Dipolar molecules tend to organize in centrosymmetric, antiparallel orientations as their respective ground states possess nonzero dipole moments; such ordering drastically diminishes bulk NLO properties relative to that which could be realized through uniform noncentrosymmetric chromophoric organization. Experimental strategies, such as dispersion of dipolar chromophores in a polymeric host material followed by electric field poling, are known to increase the degree of non-centrosymmetric chromophore orientation in bulk phase

materials; the net dipolar order achieved within such macroscopic materials using such approaches rarely exceeds that of a few percent of the total weight fraction of the chromophore present.[53−59]

Octopolar molecules, which have no permanent dipole moments and are noncentrosymmetric, may provide an approach to achieving macroscopic NLO active assemblies.[60−72] Most examples of octopolar NLO chromophores have either D_{3h} or T_d symmetry. While D_2 and D_{2d} symmetries are also appropriate for octopolar NLO chromophore designs, D_2- and D_{2d}-symmetric NLO octopoles that manifest exceptional hyperpolarizabilities are unusual.[73,74] It was shown recently that strongly coupled, D_2-symmetric oscillators designed from (porphinato)zinc(II) (PZn) and metal(II) polypyridyl (M) structural units connected via ethyne bridges define an exceptional class of octopolar NLO chromophores.[21] HRS depolarization experiments demonstrated that the measured hyperpolarizabilities (β_{HRS} values, where $\beta_{HRS}^2 = [\langle\beta_{zzz}^2\rangle + \langle\beta_{xzz}^2\rangle] = 120/35\,\beta_{xyz}^2$ for octopolar (T_d, D_2, or D_{2d}) compounds) of these MPZnM structures arise predominantly from conformers in which torsional angles between the terpyridyl units and the PZn plane are approximately equal in magnitude and opposite in sign,[21] suggesting that modest solution-phase structural subpopulations of these MPZnM chromophores possess exceptional hyperpolarizabilities.

Here, we report a series of octopolar D_2-symmetric chromophores, based on the MPZnM motif, that demonstrate that strong electronic coupling between multiple charge-transfer oscillators can provide octopolar NLO chromophores that exhibit impressive β values at 1500 nm. While wavelengths near 1500 nm define a critically important telecommunications spectral region, no molecular chromophore has thus far been delineated that exhibits a dynamic hyperpolarizability measured at a 1.5 μm incident irradiation wavelength that exceeds 700 × 10^{-30} esu;[27,61,65,74−81] this work provides new insights into the design of octopolar NLO chromophores, and demonstrates the utility of MPZnM compositions for realizing substantial β_{HRS} values at long wavelengths.

■ RESULTS AND DISCUSSION

Design and Synthesis. RuPZnRu (**1**), P$_1$RuPZnP$_1$Ru (**2**), P$_1$RuR$_f$PZnP$_1$Ru (**3**), and 5,10-P$_1$RuR$_f$PZnP$_1$Ru (**4**) (Scheme 1) were synthesized by metal-catalyzed cross-coupling[16,32,82−89] of an appropriate 4′-brominated ruthenium bis(2,2′;6′,2″-terpyridine) synthon (RuBr or P$_1$RuBr) and a (di-*meso*-ethynylporphinato)zinc(II) (EPZnE) complex (Scheme 1). These chromophores are based on the MPZnM motif,[21,89] in which two bis(terpyridyl)metal(II) units are connected to a PZn *meso* carbon position via ethynyl connectivity. RuPZnRu, P$_1$RuPZnP$_1$Ru, P$_1$RuR$_f$PZnP$_1$Ru, and 5,10-P$_1$RuR$_f$PZnP$_1$Ru were isolated as described in the Supporting Information; tetrakis(hexafluorophosphate) salts of these chromophores were used in all the spectroscopic experiments described below.

Previous work establishes that (i) strongly coupled D_2 symmetric oscillators can provide impressive octopolar NLO chromophores, (ii) MPZnM measured hyperpolarizabilities derive largely from conformers in which the torsional angles between the terpyridyl and porphyryl units are approximately equivalent in magnitude and opposite in sign, and (iii) the observed octopolar NLO response derives from the collective response of the component dipolar RuPZn supermolecular units.[21] Compounds **1−4** provide a compact set of chromophores that probe how electronic and geometric factors

impact the measured hyperpolarizability at long irradiation wavelengths. These structures take advantage of electron-rich 10,20-diarylporphyrin (**1**, **2**) or electron-deficient 10,20-bis-(perfluoroalkyl)porphyrin frameworks (**3**, **4**), unsubstituted terpyridyl (**1**) and 4′-pyrrolidinyl-2,2′;6′,2″-terpyridyl ligands (**2**, **3**, **4**), and modulation of metal(II) polypyridyl-to-(porphinato)zinc connectivity (**3**, **4**). The bis[*meso*-(perfluoroalkyl)porphinato]zinc(II) unit provides a PZn chromophoric building block that features HOMO and LUMO levels stabilized by ∼0.3 eV relative to the corresponding orbitals of [5,15-diarylporphinato]zinc-(II);[40,90−92] this electronic structural modification of the PZn chromophore provides a convenient means to modulate the supermolecular charge resonance character that originates from M and PZn electronic and excitonic interactions that derive from the porphyrin *meso*-carbon-to-terpyridyl-carbon ethynyl linkage.[16,42] Likewise, relative to an unsubstituted terpyridyl ligand, the 4′-pyrrolidinyl substituent modulates terpyridyl ligand π^* energy levels and diminishes the $E_{1/2}(M^{3+/2+})$ value of the bis(terpyridyl)ruthenium(II) structure by 0.3 eV, regulating the respective energies of the PZn$_n$-derived $\pi \rightarrow \pi^*$ and bis(terpyridyl)metal(II) charge-transfer states.[41] Further, as both the effective chromophore optical symmetry and the nature of the dipolar coupling between independent RuPZn units in larger MPZn-based supermolecules dramatically modulate NLO response,[89] chromophores **3** and **4** provide insight on how transition dipole moment orientation influences electronic structure and the measured hyperpolarizability.[93]

Electronic Absorption and Potentiometric Data. The electronic absorption spectra (EAS) of these species (Figure 1, Table 1) indicate strong mixing of the PZn-based oscillator strength with ruthenium terpyridyl charge resonance bands.
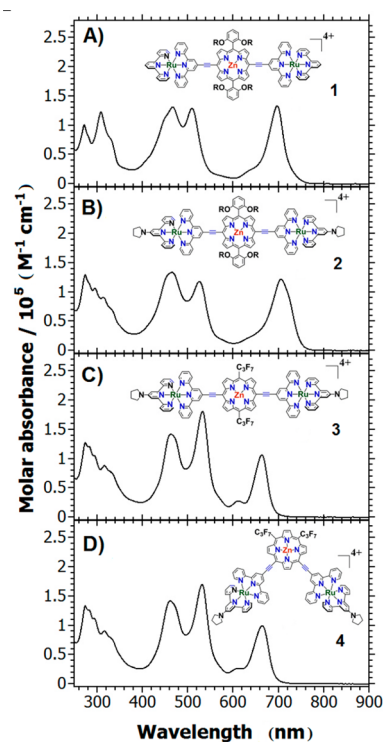

Figure 1. Electronic absorption spectra of (A) RuPZnRu, (B) P$_1$RuPZnP$_1$Ru, (C) P$_1$RuR$_f$PZnP$_1$Ru, and (D) 5,10-P$_1$RuR$_f$PZnP$_1$Ru recorded in CH$_3$CN solvent at 20 °C.

Table 1. Electronic Absorption^a and Potentiometric Data^b for Compounds 1−4

	abs band maxima [nm] ($\varepsilon/10^5$ [M^{-1} cm^{-1}])			potentiometric data (mV)				
	B band	^{1}MLCT	Q bands	ZnP$^{0/+}$	ZnP$^{+/2+}$	M$^{2+/3+}$	tpy$^{-/0}$	ZnP$^{-/0}$
RuPZnRu (1)^{c,d}	467 (1.31)	510 (1.29)	697 (1.33)	920	1155	1450	−895	−1330
P$_1$RuPZnP$_1$Ru (2)^e	466 (1.33)	525 (1.18)	706 (1.22)	855	1195	980	−925	−1410
P$_1$RuR$_f$PZnP$_1$Ru (3)^e	463 (1.42)	533 (1.80)	612 (0.28)	1380		975	−755	−965
			663 (1.06)					
5,10-P$_1$RuR$_f$PZnP$_1$Ru (4)^e	462 (1.42)	532 (1.70)	612 (0.26)	1405		970	−690	−1030
			664 (0.99)					

^{a}All absorption spectra were recorded in CH_3CN; [chromophore] = 1 μM. ^{b}Experimental conditions: [chromophore] = 1−4 mM; scan rate = 0.5 V/s; reference electrode = Ag/AgCl; working electrode = Pt disk. $E_{1/2}$ values are reported relative to SCE; the ferrocene/ferrocenium couple (0.43 V vs SCE) was used as an internal standard. ^{c}Potentiometric data recorded in 0.1 M TBAPF$_6$/DMF electrolyte/solvent system. ^{d}Taken from refs 42 and 95. ^{e}Potentiometric data recorded in 0.1 M TBAPF$_6$/CH$_3$CN electrolyte/solvent system.
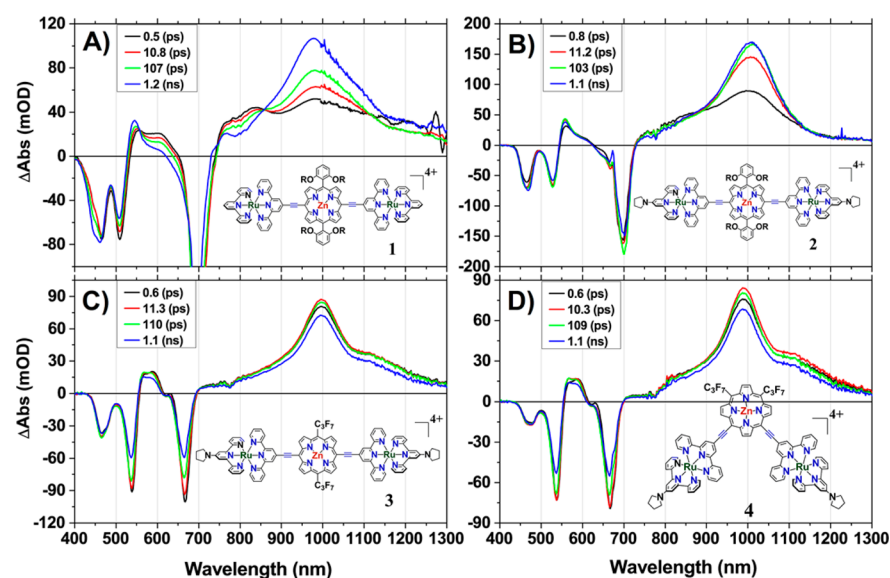

Figure 2. Representative magic angle femtosecond transient absorption spectra recorded for (A) RuPZnRu, (B) P$_1$RuPZnP$_1$Ru, (C) P$_1$RuR$_f$PZnP$_1$Ru, and (D) 5,10-P$_1$RuR$_f$PZnP$_1$Ru at time delays noted. Experimental conditions: λ_{ex} = (A) 695 nm, (B−D) 672 nm; pump energy = ∼0.5 μJ/pulse; solvent = acetonitrile; T = 20 °C.

Note that EAS of **1**−**4** differ markedly from the EAS acquired for their respective ethynyl-PZn and (terpyridyl)ruthenium building blocks (see Figure S1). It is important to note in this regard that supermolecular chromophores **1**−**4** retain spectroscopic qualities that trace their origin to those of well-studied PZn and [Ru(tpy)$_2$]$^{2+}$ oscillators. For instance, **1**−**4** show (i) strong, porphyrin B-state derived (ε > 100,000 M^{-1} cm^{-1}) absorptions near 460 nm; (ii) visible bands centered at ∼525 nm that feature (terpyridyl)metal-to-ligand singlet charge transfer (^{1}MLCT) character and porphyrin ligand oscillator strength contributions; and (iii) bands localized between 600 and 700 nm that exhibit both porphyrinic $^1\pi-\pi^*$ Q-state and charge resonance character that derive from conjugation expansion[10,15,94] and the strong electronic coupling between the (porphinato)metal and (terpyridyl)metal units.[16,42] In order to simplify comparison of the spectral properties of these conjugated supermolecules with those of common porphyrin and (terpyridyl)metal(II) benchmarks, we preserve MLCT (d−π^*), Soret (B)-band, and Q-band ($\pi-\pi^*$) transition labels. When these terms are used in reference to the absorptions of MPZnM chromophores, they denote only the dominant contributor to the oscillator strength of the specific transition, as MLCT, ligand, Soret, and Q electronic states are extensively mixed in these supermolecules.

Figure 1 shows that, for all of these compounds, dramatic oscillator strength transfer from the B band to the Q band arises from the coupling between two chromophoric units. Despite significant modulation of the ruthenium oxidation potential (Table 1), incorporation of a pyrrolidine donor on the metal complex has little effect on the ground-state electronic absorption spectrum, because the moderate intensity ^{1}MLCT transition is buried underneath the strong porphyrin-derived $S_0 \rightarrow S_2$ absorption manifold, as is evident from spectra recorded for compounds **1** and **2**. Changing PZn ancillary 10,20-meso substitution from an electron rich 3,5-bis(3,3-dimethyl-1-butyloxy)phenyl to an electron deficient heptafluoropropyl group (compare structures of compounds **2** and **3**; Figure 1B,C) substantially blue shifts (∼850 cm^{-1}) the low energy Q-state-derived absorption band maximum. Note also that substitution of the PZn ancillary meso aryl moiety with a perfluoroalkyl substituent (Figure 1 C,D) drives increased porphyrin ligand oscillator strength contributions to the transition manifold centered near 525 nm, which features augmented metal-to-ligand charge transfer character relative to that observed for compounds **1** and **2** (Figure 1A,B). Potentiometric data for supermolecular chromophores **1**−**4** are compiled in Table 1.

Excited-State Dynamics. Pump−probe transient absorption spectroscopic studies of **1**−**4** demonstrate excited-state dynamical characteristics and transient spectral features closely related to those reported for the archetypal dipolar supermolecular donor−acceptor ruthenium(II) [5-(4′-ethynyl-(2,2′;6′2″-terpyridinyl))-10,20-bis(2′,6′-bis(3,3-dimethyl-1-butyloxy)phenyl)porphinato]zinc(II)-(2,2′;6′,2″-terpyridine)$^{2+}$ bis(hexafluorophosphate) chromophore, RuPZn (Scheme 1).[41,42,89] In this respect, it is important to appreciate that the excited-state relaxation dynamics of RuPZn and related chromophores[41,42] exhibit significant departures from those characteristic of simple (porphinato)metal and (terpyridyl)metal species. Monomeric (porphinato)zinc(II) species relax typically through both the singlet and triplet manifolds, leading to nanosecond (singlet) and millisecond (triplet) deactivation time scales;[31] at room temperature, the initially prepared [Ru(tpy)]$^{2+}$ electronically excited state relaxes rapidly to the low-lying metal-to-ligand charge transfer (triplet) surface,[96−98] where fast intersystem crossing dynamics are driven by thermal population of a low-lying ^{3}MC state, resulting in a ^{3}MLCT lifetime of only a few hundred picoseconds at 298 K.[99] In RuPZn,[41,42] transient absorption spectra obtained at early time delays (t_{delay} < 400 fs) demonstrate fast excited-state relaxation and formation of a highly polarized T$_1$ excited state; the combined effects of rapid intersystem crossing and strong coupling to low-lying MLCT states gives rise to excited-state lifetimes >10 μs, and a negligible excite-state population loss to ground-state on the intersystem crossing time scale (τ_{isc} ~ 4 ps) following S$_0$ → S$_1$ excitation. Pump−probe transient optical spectroscopic and dynamical investigations of RuPZn electronically excited states reveal prominent spectral characteristics that include (i) visible spectral domain bleaching due to ground-state depletion, (ii) a broad, weak transient absorption in the spectral region between the B- and Q-state ground-state bleaches, and (iii) an unusually broad, intense T$_1$ → T$_n$ absorption manifold that spans the 800−1200 nm spectral range.[41,42]

Figure 2 highlights transient absorption spectral data for chromophores **1**−**4** obtained over a 200 fs-to-1 ns time domain. The transient absorption signals observed at the earliest time delays over the 700−900 nm spectral region suggest that initially prepared excited states for compounds **1**−**4** are less conjugated than their respective corresponding relaxed excited states. Supermolecules **1** and **2** manifest an ~15 ps time constant component that leads to an increase in the intensity of the T$_1$ → T$_n$ NIR transient absorption manifold; these dynamics are associated with torsional motion about the ethynyl bridge.[33,41,42,100] Global analysis of the excited-state transient dynamical data acquired for **3** and **4** indicates an ultrafast relaxation process ($\tau_{relaxation}$ < 1 ps) that leads to an increase in the intensity of the T$_1$ → T$_n$ NIR transient absorption band. This effect likely derives from the electronic structure of the bis[*meso*-(perfluoroalkyl)porphinato]zinc(II) units of **3** and **4**: as the potentiometrically determined HOMO levels of these electron deficient PZn chromophoric building blocks are stabilized by ~0.3 eV relative to the corresponding orbitals of [*meso*-arylporphinato]zinc(II),[40,90−92] enhanced ground-state charge-resonance interactions between the metal terpyridyl and PZn units drive reduced torsional angle conformational heterogeneity between the porphyryl and terpyridyl least-squares planes relative to that exhibited by **1** and **2**. The more planar, conformationally uniform nature of the chromophore **3** and **4** ground states relative to those of **1**

and **2** is thus reflected in their order-of-magnitude diminished $\tau_{relaxation}$ values, as their mean terpyridyl-(porphinato)metal torsional angles more closely resemble those of their respective relaxed electronically excited states.[41,42]

Figures 3 and S2 highlight transient absorption spectral data acquired for chromophores **1**−**4** over ns-to-μs time domains;
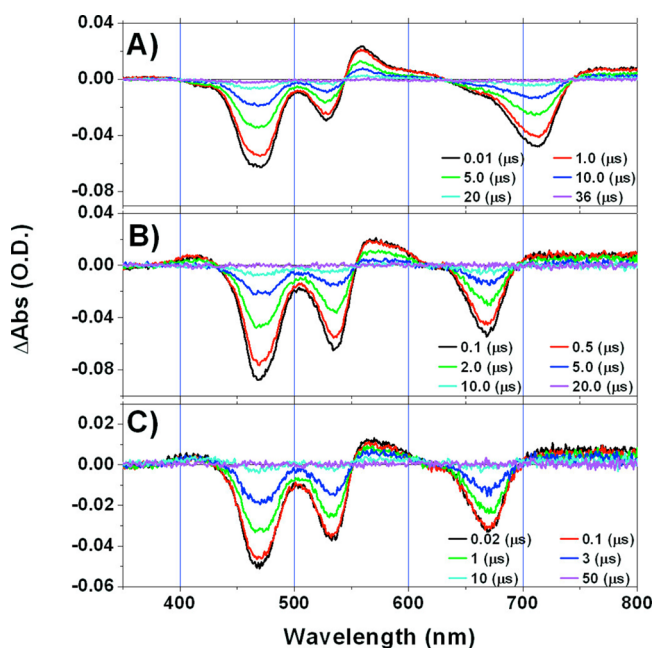

Figure 3. Nanosecond pump−probe transient absorption spectra of (A) P$_1$RuPZnP$_1$Ru (**2**), (B) P$_1$RuR$_f$PZnP$_1$Ru (**3**), and (C) 5,10-P$_1$RuR$_f$PZnP$_1$Ru (**4**) recorded at time delays noted. Experimental conditions: solvent = deaerated acetonitrile; λ_{ex} = 532 nm; pump energy =1−3 mJ/pulse; ambient temperature.

Table 2. Electronically Excited Triplet State Spectral Data^a for Compounds 1−4

chromophore	λ_{max} (T$_1$ → T$_n$)^b (nm)	ε/10^5 M^{-1} cm^{-1} (T$_1$ → T$_n$)^c	τ_T (μs)^d
RuPZnRu (**1**)	980^e	1.48	10.4^e
P$_1$RuPZnP$_1$Ru (**2**)	1006	1.32	9.0
P$_1$RuR$_f$PZnP$_1$Ru (**3**)	996	1.22	3.3
5,10-P$_1$RuR$_f$PZnP$_1$Ru (**4**)	988	1.14	3.3

^{a}All spectral data were acquired in acetonitrile solvent. $^b\lambda_{max}$ (T$_1$ → T$_n$) values were determined from transient absorption spectra recorded at a 1 ns time delay. ^{c}The excited-state extinction coefficients were estimated using a method described previously;[42] reported values were determined at the T$_1$ → T$_n$ λ_{max}. ^{d}The triplet-state lifetimes were determined using μs time domain transient absorption measurements carried out in dry dearated acetonitrile solvent. $^e\lambda_{max}$ (T$_1$ → T$_n$) and triplet lifetime were reported previously.[42]

Table 2 tabulates excited-state lifetimes, T$_1$ → T$_n$ absorption maxima, and T$_1$ → T$_n$ absorption extinction coefficients for these compounds. Note that these estimated T$_1$ → T$_n$ extinction coefficients (ε~ 10^5 M^{-1} cm^{-1}) are calculated from fs transient absorption spectra acquired at 1 ns following excitation, and were estimated by comparing the excited-state absorption to the Q$_x$-band derived ground-state bleach (having a known extinction coefficient), following a method detailed

Table 3. Dynamic Hyperpolarizabilities [β_{HRS}, ($\times 10^{-30}$ esu)][a] and Depolarization Ratios (ρ) Determined from Hyper-Rayleigh Experiments

	800 nm	840 nm	1064 nm	1300 nm	1320 nm	1340 nm	1500 nm	ρ[b]
RuPZn[c]	200 ± 30	700 ± 100		1300 ± 100	1320 ± 70	90 ± 40	110 ± 4	3.8
RuPZnRu (**1**)	190 ± 30	450 ± 70	1000 ± 100	260 ± 80	660 ± 40	710 ± 40	4600 ± 1200	1.7
P$_1$RuPZnP$_1$Ru (**2**)	220 ± 10	510 ± 80	300 ± 40		180 ± 70		600 ± 100	1.9
P$_1$RuR$_f$PZnP$_1$Ru (**3**)	180 ± 10	390 ± 60					30 ± 4	1.8

[a]Total HRS intensity as noted in the text at the indicated wavelength. [b]Measured at λ_{inc} = 800 nm. [c]Hyperpolarizability values for RuPZn have been reported previously.[16,22] A blank entry indicates a β_{HRS} value <30 × 10^{-30} esu.

previously.[42] Note that $\lambda_{max}(T_1 \rightarrow T_n)$ increases modestly with incorporation of the pyrrolidine group on the terpyridyl ligand (**1**, $\lambda_{max}(T_1 \rightarrow T_n)$ = 980 nm; **2**, $\lambda_{max}(T_1 \rightarrow T_n)$ = 1006 nm), congruent with enhanced electronic delocalization within the compound **2** T_1 state. Note also that relative to **1**, the enhanced ground-state charge-resonance interactions between the metal terpyridyl and PZn units of chromophores **3** and **4** that derive from the electron-deficient perfluoroalkyl-substituted porphyrin macrocycle result also in red-shifted $\lambda_{max}(T_1 \rightarrow T_n)$ values (**3**, $\lambda_{max}(T_1 \rightarrow T_n)$ = 996 nm; **4**, $\lambda_{max}(T_1 \rightarrow T_n)$ = 988 nm). In sum, Figures 2 and 3 and Table 2 data underscore that the combination of fast intersystem crossing, long triplet-state lifetimes, and unusually large $\varepsilon(T_1 \rightarrow T_n)$ values make chromophores **1**−**4** exceptional excited-state absorbers for this region of the NIR.

Nonlinear Optical Properties. For chromophores with charge transfer (CT) transitions that dominate the NLO response, the dynamic hyperpolarizability can be approximated using a two-state description of β (eq 1).

$$\beta_n' = \frac{6(P_{ge})_n^2 (\Delta\mu_{ge})_n (E_{op})_n^2}{[(E_{op})_n^2 - (2E_{inc})^2][(E_{op})_n^2 - E_{inc}^2]} \quad (1)$$

Here, P_{ge} is the oscillator strength for the CT transition, $\Delta\mu_{ge}$ the dipole moment difference between ground and CT excited states, E_{op} the energy gap between the two states, and E_{inc} the incident irradiation energy.[101,102] Within the limited context of a single two-level model for charge transfer (along the molecular z-axis) dominated dipolar molecules, β_n' is an excellent approximation for β_{zzz}. Dipolar RuPZn-based chromophores are characterized by large CT transition oscillator strengths (P_{ge}s), and significant dipole-moment differences between the ground and excited electronic states ($\Delta\mu_{ge}$s). These species exhibit complicated nonlinear responses because of two- and three-level contributions arising from mixing of transitions that possess (porphinato)zinc B-, (porphinato)zinc Q-, and ruthenium-to-ligand (MLCT)-state character, and the fact that these transitions have $\Delta\mu_{ge}$s with both positive and negative sign.[16,22,41]

A two-state model to describe the electronic hyperpolarizability is appealing for its simplicity and qualitative description of the underlying physical principles. The direct linkage to experimental data, namely, transition dipole moments, optical transition energies, and energy detunings from resonance, is particularly appealing. While of qualitative use for exploring structure−hyperpolarizability relationships, the two-level model does not describe the frequency dispersion of the hyperpolarizability with quantitative accuracy. We recently developed and used generalized Thomas−Kuhn sum (TKS) rules to describe the frequency-dependent hypolarizabilities in a manner that retains the appealing simplicity and direct linkage to linear absorption spectra, while incorporating the influence

of multiple excited states that contribute to the hyperpolarizability. Within this framework, a satisfactory description was found for the frequency dispersion of the hyperpolarizabilities for dipolar chromophores.[22] Here, we use this approach to describe qualitatively octopolar chromophores with more than two excited states that contribute to the irradiation-wavelength dependent hyperpolarizability. Since multiple absorption manifolds contribute to the nonlinear response in RuPZn-based chromophores, and the transitions that dominate these manifolds possess distinct transition dipole directions, octopolar chromophores **1**−**4** are anticipated to exhibit complex hyperpolarizability spectra.

Table 3 lists dynamic hyperpolarizability (β_λ) values for compounds **1**−**3**, determined from hyper-Rayleigh light scattering (HRS) measurements carried out at different incident irradiation wavelengths (λ_{inc}s) in CH$_3$CN solvent. The total HRS intensities listed in Table 3 (i.e., the total magnitude of the HRS signal with polarization parallel and perpendicular to the Z-polarized fundamental laser beam, $\beta_{HRS}^2 = [\langle\beta_{zzz}^2\rangle + \langle\beta_{xzz}^2\rangle]$) provide an average hyperpolarizability value that has not been separated into specific hyperpolarizability tensor components for a specific molecular symmetry.[103,104] For chromophores **1**−**3**, hyperpolarizabilities were measured at multiple incident wavelengths, producing a "hyperpolarizability spectrum"; such data are important, as these may be used in combination with appropriate theoretical frameworks to identify electronic states that contribute to the NLO response at a specific λ_{inc}, and thereby provide chromophore design insights necessary to optimize the hyperpolarizability at the frequency of interest. Table 3 reports irradiation wavelength-dependent measured hyperpolarizabilities for RuPZnRu (**1**), P$_1$RuPZnP$_1$Ru (**2**), P$_1$RuR$_f$PZnP$_1$Ru (**3**), and the dipolar RuPZn benchmark.

As a case in point, note that RuPZnRu (Table 3) displays a complex hyperpolarizabilty dispersion: at λ_{inc} = 800 nm, the measured hyperpolarizability (β_{800} = 190 ± 30 × 10^{-30} esu) is modest. The magnitude of β_λ increases as the irradiation wavelength is tuned to 840 and 1064 nm (β_{840} = 450 ± 70 × 10^{-30} esu; β_{1064} = 1000 ± 100 × 10^{-30} esu), decreases as λ_{inc} moves further to the red (β_{1300} = 260 ± 80 × 10^{-30} esu), increases steadily at slightly longer irradiation wavelengths (β_{1320} = 660 ± 40 × 10^{-30} esu; β_{1340} = 710 ± 40 × 10^{-30} esu), but increases dramatically at λ_{inc} = 1500 nm (β_{1500} = 4600 ± 1200 × 10^{-30} esu). This β_{HRS} value is the largest yet reported for any chromophore at λ_{inc} = 1500 nm.

Table 3 further tabulates depolarization ratio measurements determined at λ_{inc} = 800 nm. The depolarization ratio, ρ, is the ratio of the HRS signal intensity (I) parallel to ($I_\parallel$) and perpendicular to ($I_\perp$) the incident polarization ($\rho = I_\parallel/I_\perp = \langle\beta_{zzz}^2\rangle/\langle\beta_{xzz}^2\rangle$). HRS depolarization ratio measurements provide information regarding the optical symmetry of states that give rise to the NLO response. For a classic dipolar NLO
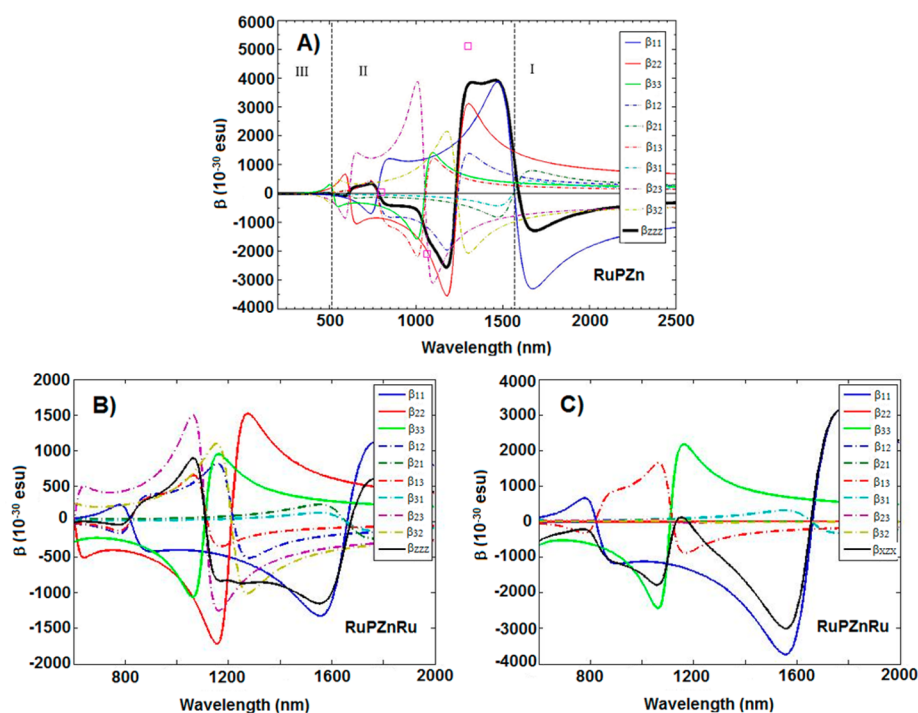
Figure 4. Comparison of the computed hyperpolarizability tensors β_{zzz} for (A) RuPZn and (B) RuPZnRu, and (C) β_{xzx} for RuPZnRu. The two-level contribution from the Q_x-derived transition is β_{11}; the two-level contribution from the ^{1}MLCT-derived transition is β_{22}; the two-level contribution from the B-derived transition is β_{33}; β_{12}, β_{21}, β_{13}, β_{31}, β_{23}, and β_{32} are the three-level contributions from the coupling of ^1Q_x-, ^{1}MLCT-, and B-derived excited states. See the Supporting Information for further details.

chromophore such as disperse red 1, $\rho = 3.4$; for an octopolar NLO chromophores such as 1,3,5-trihydroxy-2,4,6-trinitrobenzene and crystal violet, $\rho = 1.5$. Measured depolarization ratios for chromophores **1−3** are ~1.8; these data, in combination with the chemical topology of the structures, are congruent with the D_2 octopolar nature of these structures.

Thomas−Kuhn Sum-over-States (TKS) Analysis. A central goal in nonlinear optics is to establish conceptual frameworks to understand and to tune the hyperpolarizability and frequency dependant nonlinear response. Addressing these design challenges in the frequency domain is especially significant since NLO devices function at finite wavelengths, making it difficult to generalize design-response principles that may be established at either shorter or longer wavelengths. Nonetheless, quantum chemical analysis[15,105−113] can be of great value in the regime of nonzero frequency. Developing predictive methods to describe β_λ remains an open challenge.[114] One bottleneck to predicting β_λ is the inclusion of multiple excited states that impact the electronic hyperpolarizability. Excitation energies, the transition moments, basis set, treatment of solvation, and level of electronic structure theory are all well-known to influence the computed nonlinear electronic response. Prior studies[9,16,115] have interpreted β_λ qualitatively in the context of the two electronic state model (eq 1). This model includes resonant enhancement from one and two photon resonant terms. The excitation energies and the oscillator strengths are provided by the linear absorption spectra. However, the data derived from linear spectra are not adequate to make predictions of hyperpolarizabilities. The reason is that the linear absorption spectra lack transition dipole moment information linking multiple excited states, and this information is needed for three-state (or higher) β_λ computation.

We recently showed that the generalized Thomas−Kuhn sum (TKS) rules may be used to compute the effective excited-state-to-excited-state transition dipole moments (within a few-state model) using the experimental linear-absorption spectra. These data can then be used to estimate the hyperpolarizabilities as a function of frequency, including two- and three-state contributions for RuPZn and related dipolar chromophores.[22] TKS analysis uses linear-absorption data to extract the transition dipoles and energies of a small number of "effective" excited electronic states, thus providing key input data required to compute β_λ (Supporting Information). Our earlier studies found that while structures may possess similar absorption spectra, the frequency-dependent hyperpolarizabilities may be very different because of differences in the influence of excited-state-to-excited-state transition moments.

The TKS analysis enables the use of linear optical absorption spectra and a few hyperpolarizability measurements to estimate the full frequency-dependent NLO response for RuPZn and related dipolar chromophores. Nonetheless, it is critical to recognize that the octopolar D_2 symmetric structure for chromophores **1−3** requires that both β_{zzz} and β_{xzx} tensors be computed, making a corresponding TKS analysis of the NLO octopole structures of current interest more complex than those modeled earlier. The fact that the present analysis includes only a limited number of effective excited states makes the octopolar NLO analysis described here more qualitative than that of our earlier studies.

With these caveats in mind, we performed a basic TKS analysis for the RuPZnRu chromophore using its linear-absorption spectrum and the frequency-dependent hyperpolarizability data compiled in Table 3. As β_{zzz} and β_{xzx} tensor components play key roles in determining the hyperpolarizability spectrum for RuPZnRu, Figure 4 compares the

computed wavelength-dependent contributions of these tensor components relative to the computed β_{zzz} tensor contribution for RuPZn (Figure 4A),[22] which largely determines the β_λ spectrum for the dipolar benchmark RuPZn. Figure 4B,C shows the frequency-dependent two- and three-state computed contributions to β_{zzz} and β_{xzx} values for RuPZnRu. These data indicate that, for RuPZnRu, the two- and three-state contributions to β_{zzz} are of smaller magnitude over the entire hyperpolarizability spectrum compared to that computed for RuPZn. This finding underscores the fact that off-diagonal beta tensor components are of critical importance in determining the hyperpolarizability spectrum of octopolar molecules. Congruent with experiment, the TKS computed β_{zzz} value for RuPZn is large at ~1300 nm. Similarly, the corresponding calculated β_{zzz} and β_{xzx} contributions for RuPZnRu at λ_{inc} = 1300 nm are modest, in line with experimental data (Table 3). Note, however, that both the β_{zzz} and β_{xzx} frequency dependent tensor elements for RuPZnRu reach maxima near 1550 nm, in agreement with the observed large β_{HRS} value (4600 ± 1200 × 10^{-30} esu; Table 3) measured for this chromophore at 1500 nm. At this level of analysis, the TKS rules indicate that relative to analogous dipolar chromophores, octopolar supermolecules will be likely characterized by more intricate dependences of the measured hyperpolarizability upon irradiation wavelength due to the interactions among multiple different β tensor components.

EXPERIMENTAL SECTION

Materials and Instrumentation. Inert atmosphere manipulations were carried out under argon prepurified by passage through an O_2 scrubbing tower (Schweizerhall R3-11 catalyst) and a drying tower (Linde 3 Å molecular sieves). Air-sensitive solids were handled in a Braun 150-M glovebox. Standard Schlenk techniques were employed to manipulate oxygen and moisture sensitive chemicals. ACS grade $CHCl_3$, CH_2Cl_2, CH_3CN, and hexanes solvents were purchased from Fisher Scientific. Tetrahydrofuran (Fisher Scientific, HPLC grade) was either distilled from potassium/benzophenone or purified using an Innovative Technology Puresolv solvent purification system. Triethylamine was distilled from CaH_2; acetonitrile was purified by distillation from CaH_2. $Pd(PPh_3)_4$, $PdCl_2(PPh_3)_2$, $Pd_2(dba)_3$, and CuI were obtained from either Aldrich or Strem Chemicals. All other commercially available reagents were used as received. An inert atmosphere was maintained in all reactions unless otherwise stated. Chromatographic purification (silica gel, 60 Å pore size, 230−400 mesh, EM Scientific or Silicycle) of all newly synthesized compounds was accomplished on the benchtop. All NMR solvents were used as received. Chemical shifts for ^1H NMR spectra are relative to the internal reference (tetramethylsilane) in $CDCl_3$, or solvent residual protium (acetonitrile-d_3, δ = 1.93 ppm, THF-d_8, δ = 1.85, 3.76 ppm). The number of attached protons and coupling constants are found in parentheses following the chemical shift values. Laboratory instrumentation has been described previously.[89]

Ultrafast Transient Absorption Experiments. Instrumentation used to acquire ultrafast transient absorption spectra has been described previously.[41,89,116] Samples for these studies were prepared, manipulated, and handled as described earlier.[41,89] Following acquisition of pump−probe spectroscopic data, linear absorption spectroscopy confirmed that all samples investigated were robust.

Nanosecond Transient Absorption Experiments. Nanosecond transient absorption spectra were acquired utilizing an Edinburgh Instruments LP920 laser flash photolysis spectrometer and Edinburgh L900 Software. Pump pulses were generated from a Q-switched Nd:YAG laser (Quantel, Brillant) and a dual-crystal OPO (OPOTEK, Vibrant LDII). The temporal width of the pump pulses was ~5 ns; the energy of the pulses exiting the OPO was controlled using neutral density filters. A Xe flash lamp was used as a white light probe source, and a CCD array detector enabled acquisition of transient data over the 185−875 nm wavelength domain. Both the LP920 and Opotek OPO are computer interfaced and controlled by the L900 software. Transient spectra reported derive from data acquired over ~20−50 scans. Samples were prepared in 1 cm quartz cells and deaerated by 3 freeze−pump−thaw cycles prior to excitation. Excited-state lifetimes were calculated via monoexponential fitting using Origin 9.1 software.

Hyper-Rayleigh Light Scattering (HRS) Measurements. Femtosecond HRS experiments were performed according the method published earlier.[27,117,118] The main difference with respect to previous studies involves the spectral domain of these measurements, which included a large number of measurement wavelengths extending to 1500 nm.[16,21,89] For this extended set of wavelengths, a variety of reference compounds [crystal violet (CV; β_{800} (methanol) = 208.6 × 10^{-30} esu),[119] p-nitroaniline (pNA; β_{1064} (acetonitrile) = 8.7 × 10^{-30} esu),[120] and disperse red 1 (DR1; β_{1300} (chloroform) = 22.4 × 10^{-30} esu)][118] were used. Reference values at nearby wavelengths were derived from the two-level model. These values have been shown to provide an excellent set of self-consistent points of reference to quantitatively study the frequency dispersion of the hyperpolarizability for porphyrin-derived chromophores.[16,21,27,89,121]

The chromophores were dissolved in acetonitrile, and passed through 0.2 μm filters. For the external references in different solvents, standard local field correction factors were applied $\left(\frac{n_D^2 + 2}{3}\right)^3$, where n is the refractive index of the solvent at the sodium D line (1.330 for methanol; 1.344 for acetonitrile; and 1.446 for chloroform). HRS data were acquired using procedures described previously to ensure linearity of the HRS signal and that self-absorption of the second harmonic signal was insignificant;[89] depolarization ratios were likewise determined using approaches detailed in earlier work.[89]

Chromophore Synthesis. An exemplary synthesis of bisruthenium(II) 5,15-bis[4′-ethynyl-(2,2′;6′,2″-terpyridinyl)]-bis[10,20-bis(2′,6′-bis(3,3-dimethyl-1-butyloxy)phenyl)porphinato]zinc(II)-bis(4′-pyrrolidin-1-yl-2,2′;6′2″-terpyridine) tetrakis(hexafluorophosphate) (P₁RuPZnP₁Ru, **2**) follows below. Synthetic procedures and characterization data for all other compounds may be found in the Supporting Information.

Bisruthenium(II) 5,15-Bis[4′-ethynyl-(2,2′;6′,2″-terpyridinyl)]bis[10,20-bis(2′,6′-bis(3,3-dimethyl-1-butyloxy)phenyl)porphinato]zinc(II)-bis(4′-pyrrolidin-1-yl-2,2′;6′2″-terpyridine) Tetrakis(hexafluorophosphate) (P₁RuPZnP₁Ru, 2). [5,15-Diethynyl-10,20-bis[2′,6′-bis(3,3-dimethyl-1-butyloxy)phenyl]porphinato]zinc (50 mg, 0.0513 mmol) and ruthenium-(II) (4′-bromo-2,2′;6′,2″-terpyridine)(4′-pyrrolidin-1-yl-2,2′;6′,2″-terpyridine)bis(hexafluorophosphate) (P₁RuBr) (Scheme 1, 115 mg, 0.1143 mmol) were placed into a 100 mL Schlenk tube with a stir bar. Trisdibenzylideneacetone

dipalladium(0) (7 mg, 7.7 μmol) and triphenylarsine (31 mg, 0.1013 mmol) were added. A solvent mixture of dry THF (12 mL), CH_3CN (24 mL), and Et_3N (4 mL) was completely degassed via three freeze−pump−thaw cycles and added to the Schlenk tube. The reaction mixture was then stirred under argon atmosphere at 55 °C for 16 h, following which it was cooled to room temperature and the solvent evaporated. The residue was purified by column chromatography on silica gel, eluted with a mixed solvent of $CH_3CN:H_2O$:saturated aqueous KNO_3 = 90:9:1. The major red-brown band was collected and the solvent evaporated. The residual dark brown solid was dissolved in a minimum volume of CH_3CN, and excess ammonium hexafluorophosphate and H_2O were added. A dark brown precipitate (**2**, 110 mg, 0.0389 mmol, 76% yield based on initial bis-ethynyl porphyrin) was collected by filtration. ¹H NMR (CD_3CN): δ 9.77 (d, J = 4.5 Hz, 4H), 9.14 (s, 4H), 8.75 (d, J = 4.5 Hz, 4H), 8.58 (d, J = 8.0 Hz, 4H), 8.30 (d, J = 8.0 Hz, 4H), 7.84 (t, J = 7.0 Hz, 4H), 7.70−7.63 (m, 10H), 7.39 (d, J = 5 Hz, 4H), 7.21 (d, J = 5 Hz, 4H), 7.12 (t, J = 6 Hz, 4H), 6.99 (d, J = 8.5 Hz, 4H), 6.92 (t, J = 6 Hz, 4H), 3.83 (t, J = 7 Hz, 8H), 3.63 (s, 8H), 2.07 (s, 8H), 0.66 (t, J = 7 Hz, 8H), 0.03 (s, 36 H). Vis (CH_3CN): λ_{max} [nm] (ε [$\times 10^{-5}$ M^{-1} cm^{-1}]) 465 (1.33), 525 (1.18), 705 (1.22). MS (MALDI-TOF) m/z: 2385 (calcd for $C_{128}H_{122}F_6N_{18}O_4PRu_2Zn$ (M − 3PF_6)$^+$ 2387), 2528 (calcd for $C_{128}H_{122}F_{12}N_{18}O_4P_2Ru_2Zn$ (M − 2PF_6)$^+$ 2532), and 2674 (calcd for $C_{128}H_{122}F_{18}N_{18}O_4P_3Ru_2Zn$ (M − PF_6)$^+$ 2678).

CONCLUSION

Octopolar D_2-symmetric chromophores, based on the MPZnM motif in which (porphinato)zinc(II) (PZn) and ruthenium(II) polypyridyl (M) structural units are connected via ethyne linkages, were probed using linear and nonlinear optical spectroscopic methods to determine how electronic and geometric factors impact measured hyperpolarizabilities. Linear electronic spectra of these RuPZnRu, $P_1RuPZnP_1Ru$, $P_1RuR_fPZnP_1Ru$, and 5,10-$P_1RuR_fPZnP_1Ru$ chromophores (Figure 1) display (i) strong, porphyrin B-state derived (ε > 100,000 M^{-1} cm^{-1}) absorptions near 460 nm; (ii) visible bands centered at ~525 nm, that feature (terpyridyl)metal-to-ligand singlet charge transfer (¹MLCT) and porphyrin ligand oscillator strength contributions; and (iii) high oscillator strength absorption manifolds in the 600−700 nm range that exhibit both porphyrinic $^1\pi-\pi^*$ Q-state and charge resonance character that derive from conjugation expansion[10,15,94] and the strong electronic coupling between the (porphinato)metal and (terpyridyl)metal units. Transient absorption spectra obtained at early time delays (t_{delay} < 400 fs) demonstrate fast excited-state relaxation, and formation of a highly polarized T_1 excited state; the T_1 states of these chromophores exhibit a broad, intense $T_1 \rightarrow T_n$ absorption manifold over the 800−1200 nm spectral domain, long (μs) triplet-state lifetimes, and unusually large NIR absorptive extinction coefficients [$\varepsilon(T_1 \rightarrow T_n) \sim 10^5$ M^{-1} cm^{-1}].

Dynamic hyperpolarizability (β_λ) values were determined from hyper-Rayleigh light scattering (HRS) measurements carried out at multiple incident irradiation wavelengths spanning the 800−1500 nm spectral domain. These RuPZn-based octopolar chromophores feature complex hyperpolarizability spectra, as (i) multiple transitions contribute to the nonlinear response and (ii) the dipole directions of these directions may be of identical or opposite sign. The measured β_{HRS} value for one of these complexes, RuPZnRu, is the largest yet reported for any chromophore at λ_{inc} = 1500 nm (4600 ± 1200 × 10^{-30} esu), highlighting that engineering of strong electronic coupling between multiple charge-transfer oscillators provides a critical design strategy to realize octopolar NLO chromophores that exhibit impressive β_{HRS} values at long, telecom-relevant wavelengths.

Generalized Thomas−Kuhn sum (TKS) rules were used to compute the effective excited-state-to-excited-state transition dipole moments from experimental linear-absorption spectra; these data were then utilized to compute hyperpolarizabilities as a function of frequency, that include two- and three-state contributions for both the β_{zzz} and β_{xzx} tensor components to the RuPZnRu hyperpolarizability spectrum. This qualitative analysis shows that the β_{zzz} and β_{xzx} tensor contributions to the RuPZnRu hyperpolarizability spectrum reach maxima near 1550 nm, in agreement with experimental data. This qualitative TKS analysis finds that octopolar molecules will be likely characterized by more intricate dependences of the measured hyperpolarizability upon irradiation wavelength due to the interactions among multiple different β tensor components.

ASSOCIATED CONTENT

Supporting Information

The Supporting Information is available free of charge on the ACS Publications website at DOI: 10.1021/acscentsci.6b00291.

> Characterization, electrochemical, and computational data, experimental details, and electronic absorption spectra (PDF)

AUTHOR INFORMATION

Corresponding Authors
*E-mail: david.beratan@duke.edu.
*E-mail: koen.clays@kuleuven.be.
*E-mail: michael.therien@duke.edu.

ORCID
Michael J. Therien: 0000-0003-4876-0036

Author Contributions
All authors contributed to writing this manuscript and have given their approval to the final version.

Notes
The authors declare no competing financial interest.

ACKNOWLEDGMENTS

REFERENCES

(1) Verbiest, T.; Clays, K.; Rodriguez, V. *Second-order Nonlinear Optical Characterization Techniques: An Introduction*; CRC Press: New York, 2009.

(2) Prasad, P. N.; Williams, D. J. *Introduction to Nonlinear Optical Effects in Molecules and Polymers*; Wiley: New York, 1991.

(3) Beratan, D. N. In *New Materials for Nonlinear Optics*; Hann, R. A., Bloor, D., Eds.; ACS Symposium Series 455; American Chemical Society: Washington, DC, 1991.

(4) Williams, D. J. Organic polymeric and non-polymeric materials with large optical nonlinearities. *Angew. Chem., Int. Ed. Engl.* **1984**, *23*, 690−703.

(5) Chauchard, E.; Combellas, C.; Hendrickx, E.; Mathey, G.; Suba, C.; Persoons, A.; Thiebault, A. Hyperpolarization properties of pyridinium and quinolinium salts determined by hyper-rayleigh scattering. *Chem. Phys. Lett.* **1995**, *238*, 47−53.

(6) Kang, H.; Facchetti, A.; Zhu, P.; Jiang, H.; Yang, Y.; Cariati, E.; Righetto, S.; Ugo, R.; Zuccaccia, C.; Macchioni, A.; Stern, C. L.; Liu, Z.; Ho, S.-T.; Marks, T. J. Exceptional molecular hyperpolarizabilities in twisted π-electron system chromophores. *Angew. Chem., Int. Ed.* **2005**, *44*, 7922−7925.

(7) Kang, H.; Facchetti, A.; Jiang, H.; Cariati, E.; Righetto, S.; Ugo, R.; Zuccaccia, C.; Macchioni, A.; Stern, C. L.; Liu, Z.; Ho, S.-T.; Brown, E. C.; Ratner, M. A.; Marks, T. J. Ultralarge hyperpolarizability twisted π-electron system electro-optic chromophores: synthesis, solid-state and solution-phase structural characteristics, electronic structures, linear and nonlinear optical properties, and computational studies. *J. Am. Chem. Soc.* **2007**, *129*, 3267−3286.

(8) Shi, Y.; Lou, A. J.-T.; He, G. S.; Baev, A.; Swihart, M. T.; Prasad, P. N.; Marks, T. J. Cooperative coupling of cyanine and tictoid twisted π-systems to amplify organic chromophore cubic nonlinearities. *J. Am. Chem. Soc.* **2015**, *137*, 4622−4625.

(9) Karki, L.; Vance, F. W.; Hupp, J. T.; LeCours, S. M.; Therien, M. J. Electronic stark effect studies of a porphyrin-based push-pull chromophore displaying a large first hyperpolarizability: State-specific contributions to beta. *J. Am. Chem. Soc.* **1998**, *120*, 2606−2611.

(10) LeCours, S. M.; Guan, H.-W.; DiMagno, S. G.; Wang, C. H.; Therien, M. J. Push-pull arylethynyl porphyrins: new chromophores that exhibit large molecular first-order hyperpolarizabilities. *J. Am. Chem. Soc.* **1996**, *118*, 1497−1503.

(11) Ledoux, I.; Zyss, J.; Jutand, A.; Amatore, C. Nonlinear optical-properties of asymmetric polyphenyls - efficiency versus transparency trade-off. *Chem. Phys.* **1991**, *150*, 117−123.

(12) Marder, S. R.; Cheng, L.-T.; Tiemann, B. G.; Friedli, A. C.; Blanchard-Desce, M.; Perry, J. W.; Skindhøj, J. Large first hyper-polarizabilities in push-pull polyenes by tuning of the bond length alternation and aromaticity. *Science* **1994**, *263*, 511−514.

(13) Marder, S. R.; Kippelen, B.; Jen, A. K.-Y.; Peyghambarian, N. Design and synthesis of chromophores and polymers for electro-optic and photorefractive applications. *Nature* **1997**, *388*, 845−851.

(14) Meyers, F.; Marder, S. R.; Pierce, B. M.; Brédas, J. L. Electric field modulated nonlinear optical properties of donor-acceptor polyenes: sum-over-states investigation of the relationship between molecular polarizabilities (a, b and g) and bond length alternation. *J. Am. Chem. Soc.* **1994**, *116*, 10703−10714.

(15) Priyadarshy, S.; Therien, M. J.; Beratan, D. N. Acetylenyl-linked, porphyrin-bridged, donor-acceptor molecules: A theoretical analysis of the molecular first hyperpolarizability in highly conjugated push-pull chromophore structures. *J. Am. Chem. Soc.* **1996**, *118*, 1504−1510.

(16) Uyeda, H. T.; Zhao, Y.; Wostyn, K.; Asselberghs, I.; Clays, K.; Persoons, A.; Therien, M. J. Unusual frequency dispersion effects of the nonlinear optical response in highly conjugated (polypyridyl)-metal-(porphinato)zinc(II) chromophores. *J. Am. Chem. Soc.* **2002**, *124*, 13806−13813.

(17) Verbiest, T.; Houbrechts, S.; Kauranen, M.; Clays, K.; Persoons, A. Second-order nonlinear optical materials: recent advances in chromophore design. *J. Mater. Chem.* **1997**, *7*, 2175−2189.

(18) Zhang, T.-G.; Zhao, Y.; Asselberghs, I.; Persoons, A.; Clays, K.; Therien, M. J. Design, synthesis, linear, and nonlinear optical properties of conjugated (porphinato)zinc(ii)-based donor-acceptor chromophores featuring nitrothiophenyl and nitrooligothiophenyl electron-accepting moieties. *J. Am. Chem. Soc.* **2005**, *127*, 9710−9720.

(19) Zhang, T.-G.; Zhao, Y.; Song, K.; Asselberghs, I.; Persoons, A.; Clays, K.; Therien, M. J. Electronic modulation of hyperpolarizable (porphinato)zinc(ii) chromophores featuring ethynylphenyl-, ethy-nylthiophenyl-, ethynylthiazolyl-, and ethynylbenzothiazolyl-based electron-donating and -accepting moieties. *Inorg. Chem.* **2006**, *45*, 9703−9712.

(20) LeCours, S. M.; DiMagno, S. G.; Therien, M. J. Exceptional electronic modulation of porphyrins through meso-arylethynyl groups. Electronic spectroscopy, electronic structure, and electrochemistry of [5,15-bis[(aryl)ethynyl]-10,20-diphenylporphinato]zinc(II) com-plexes. X-ray crystal structures of [5,15-bis[(4′-fluorophenyl)-ethynyl]-10,20-diphenylporphinato]zinc(II) and 5,15-bis[(4′-methoxyphenyl)ethynyl]-10,20-diphenylporphyrin. *J. Am. Chem. Soc.* **1996**, *118*, 11854−11864.

(21) Duncan, T. V.; Song, K.; Hung, S.-T.; Miloradovic, I.; Nayak, A.; Persoons, A.; Verbiest, T.; Therien, M. J.; Clays, K. Molecular symmetry and solution-phase structure interrogated by hyper-Rayleigh depolarization measurements: Elaborating highly hyperpolarizable D_2-symmetric chromophores. *Angew. Chem., Int. Ed.* **2008**, *47*, 2978−2981.

(22) Hu, X.; Xiao, D.; Keinan, S.; Asselberghs, I.; Therien, M. J.; Clays, K.; Yang, W.; Beratan, D. N. Predicting the frequency dispersion of electronic hyperpolarizabilities based on absorption data and Thomas-Kuhn sum rules. *J. Phys. Chem. C* **2010**, *114*, 2349−2359.

(23) Keinan, S.; Therien, M. J.; Beratan, D. N.; Yang, W. Molecular design of porphyrin-based nonlinear optical materials. *J. Phys. Chem. A* **2008**, *112*, 12203−12207.

(24) Reeve, J. E.; Collins, H. A.; De Mey, K.; Kohl, M. M.; Thorley, K. J.; Paulsen, O.; Clays, K.; Anderson, H. L. Amphiphilic porphyrins for second harmonic generation imaging. *J. Am. Chem. Soc.* **2009**, *131*, 2758−2759.

(25) Therien, M. J. How to improve your image. *Nature* **2009**, *458*, 716−717.

(26) Xu, T.; Wu, S. P.; Miloradovic, I.; Therien, M. J.; Blasie, J. K. Incorporation of designed extended chromophores into amphiphilic 4-helix bundle peptides for nonlinear optical biomolecular materials. *Nano Lett.* **2006**, *6*, 2387−2394.

(27) De Mey, K.; Perez-Moreno, J.; Reeve, J. E.; Lopez-Duarte, I.; Boczarow, I.; Anderson, H. L.; Clays, K. Strong wavelength dependence of hyperpolarizability in the near-infrared biological window for second-harmonic generation by amphiphilic porphyrins. *J. Phys. Chem. C* **2012**, *116*, 13781−13787.

(28) López-Duarte, I.; Reeve, J. E.; Pérez-Moreno, J.; Boczarow, I.; Depotter, G.; Fleischhauer, J.; Clays, K.; Anderson, H. L. ″Push-no-pull″ porphyrins for second harmonic generation imaging. *Chem. Sci.* **2013**, *4*, 2024−2027.

(29) Reeve, J. E.; Corbett, A. D.; Boczarow, I.; Kaluza, W.; Barford, W.; Bayley, H.; Wilson, T.; Anderson, H. L. Porphyrins for probing electrical potential across lipid bilayer membranes by second harmonic generation. *Angew. Chem., Int. Ed.* **2013**, *52*, 9044−9048.

(30) Senge, M. O.; Fazekas, M.; Notaras, E. G. A.; Blau, W. J.; Zawadzka, M.; Locos, O. B.; Ni Mhuircheartaigh, E. M. Nonlinear optical properties of porphyrins. *Adv. Mater.* **2007**, *19*, 2737−2774.

(31) Duncan, T. V.; Susumu, K.; Sinks, L. E.; Therien, M. J. Exceptional near-infrared fluorescence quantum yields and excited-state absorptivity of highly conjugated porphyrin arrays. *J. Am. Chem. Soc.* **2006**, *128*, 9000−9001.

(32) Lin, V. S.-Y.; DiMagno, S. G.; Therien, M. J. Highly conjugated, acetylenyl bridged porphyrins: new models for light-harvesting antenna systems. *Science* **1994**, *264*, 1105−1111.

(33) Rubtsov, I. V.; Susumu, K.; Rubtsov, G. I.; Therien, M. J. Ultrafast singlet excited-state polarization in electronically asymmetric ethyne-bridged bis[(porphinato)zinc(II)] complexes. *J. Am. Chem. Soc.* **2003**, *125*, 2687−2696.

(34) Angiolillo, P. J.; Susumu, K.; Uyeda, H. T.; Lin, V. S.-Y.; Shediac, R.; Therien, M. J. Trends in triplet excitation delocalization in highly conjugated (porphinato)zinc(II) arrays probed by EPR spectroscopy. *Synth. Met.* **2001**, *116*, 247−253.

(35) Duncan, T. V.; Wu, S. P.; Therien, M. J. Ethyne-bridged (porphinato)zinc(ii)-(porphinato)iron(iii) complexes: phenomenolog-ical dependence of excited-state dynamics upon (porphinato) iron electronic structure. *J. Am. Chem. Soc.* **2006**, *128*, 10423−10435.

(36) Fletcher, J. T.; Therien, M. J. Strongly coupled porphyrin arrays featuring both, π-cofacial and linear-π-conjugative interactions. *Inorg. Chem.* **2002**, *41*, 331−341.

(37) Lin, V. S.-Y.; Therien, M. J. The role of porphyrin-to-porphyrin linkage topology in the extensive modulation of the absorptive and emissive properties of a series of ethynyl- and butadiynyl-bridged bis- and tris(porphinato)zinc chromophores. *Chem. - Eur. J.* **1995**, *1*, 645–651.

(38) Shediac, R.; Gray, M. H. B.; Uyeda, H. T.; Johnson, R. C.; Hupp, J. T.; Angiolillo, P. J.; Therien, M. J. Singlet and triplet excited states of emissive, conjugated bis(porphyrin) compounds probed by optical and EPR spectroscopic methods. *J. Am. Chem. Soc.* **2000**, *122*, 7017–7033.

(39) Susumu, K.; Duncan, T. V.; Therien, M. J. Potentiometric, electronic structural, and ground- and excited-state optical properties of conjugated bis[(porphinato)zinc(II)] compounds featuring proqui-noidal spacer units. *J. Am. Chem. Soc.* **2005**, *127*, 5186–5195.

(40) Susumu, K.; Therien, M. J. Decoupling optical and potentiometric band gaps in π-conjugated materials. *J. Am. Chem. Soc.* **2002**, *124*, 8550–8552.

(41) Duncan, T. V.; Ishizuka, T.; Therien, M. J. Molecular engineering of intensely near-infrared absorbing excited states in highly conjugated oligo(porphinato)zinc-(polypyridyl)metal(II) super-molecules. *J. Am. Chem. Soc.* **2007**, *129*, 9691–9703.

(42) Duncan, T. V.; Rubtsov, I. V.; Uyeda, H. T.; Therien, M. J. Highly conjugated (polypyridyl)metal-(porphinato)zinc(ii) com-pounds: long-lived, high oscillator strength, excited-state absorbers having exceptional spectral coverage of the near-infrared. *J. Am. Chem. Soc.* **2004**, *126*, 9474–9475.

(43) Drobizhev, M.; Stepanenko, Y.; Dzenis, Y.; Karotki, A.; Rebane, A.; Taylor, P. N.; Anderson, H. L. Extremely strong near-IR two-photon absorption in conjugated porphyrin dimers: quantitative description with three-essential-states model. *J. Phys. Chem. B* **2005**, *109*, 7223–7236.

(44) Fisher, J. A. N.; Susumu, K.; Therien, M. J.; Yodh, A. G. One- and two-photon absorption of highly conjugated multiporphyrin systems in the two-photon Soret transition region. *J. Chem. Phys.* **2009**, *130*, 134506.

(45) Hisaki, I.; Hiroto, S.; Kim, K. S.; Noh, S. B.; Kim, D.; Shinokubo, H.; Osuka, A. Synthesis of doubly beta-to-beta 1,3-butadiyne-bridged diporphyrins: Enforced planar structures and large two-photon absorption cross sections. *Angew. Chem., Int. Ed.* **2007**, *46*, 5125–5128.

(46) Screen, T. E. O.; Thorne, J. R. G.; Denning, R. G.; Bucknall, D. G.; Anderson, H. L. Amplified optical nonlinearity in a self-assembled double-strand conjugated porphyrin polymer ladder. *J. Am. Chem. Soc.* **2002**, *124*, 9712–9713.

(47) Strzalka, J.; Xu, T.; Tronin, A.; Wu, S. P.; Miloradovic, I.; Kuzmenko, I.; Gog, T.; Therien, M. J.; Blasie, J. K. Structural studies of amphiphilic 4-helix bundle peptides incorporating designed extended chromophores for nonlinear optical biomolecular materials. *Nano Lett.* **2006**, *6*, 2395–2405.

(48) Thorley, K. J.; Hales, J. M.; Anderson, H. L.; Perry, J. W. Porphyrin dimer carbocations with strong near infrared absorption and third-order optical nonlinearity. *Angew. Chem., Int. Ed.* **2008**, *47*, 7095–7098.

(49) Zou, H.; Therien, M. J.; Blasie, J. K. Structure and dynamics of an extended conjugated NLO chromophore within an amphiphilic 4-helix bundle peptide by molecular dynamics simulation. *J. Phys. Chem. B* **2008**, *112*, 1350–1357.

(50) Raymond, J. E.; Bhaskar, A.; Goodson, T.; Makiuchi, N.; Ogawa, K.; Kobuke, Y. Synthesis and two-photon absorption enhancement of porphyrin macrocycles. *J. Am. Chem. Soc.* **2008**, *130*, 17212–17213.

(51) Clays, K.; Wostyn, K.; Olbrechts, G.; Persoons, A.; Watanabe, A.; Nogi, K.; Duan, X. M.; Okada, S.; Oikawa, H.; Nakanishi, H.; Vogel, H.; Beljonne, D.; Brédas, J.-L. Fourier analysis of the femtosecond hyper-Rayleigh scattering signal from ionic fluorescent hemicyanine dyes. *J. Opt. Soc. Am. B* **2000**, *17*, 256–265.

(52) Ma, H.; Liu, S.; Luo, J.; Suresh, S.; Liu, L.; Kang, S. H.; Haller, M.; Sassa, T.; Dalton, L. R.; Jen, A. K.-Y. Highly efficient and thermally stable electro-optical dendrimers for photonics. *Adv. Funct. Mater.* **2002**, *12*, 565–574.

(53) Dalton, L. Nonlinear optical polymeric materials: from chromophore design to commercial applications. *Adv. Polym. Sci.* **2002**, *158*, 1–86.

(54) Dalton, L. R.; Harper, A. W.; Robinson, B. H. The role of London forces in defining noncentrosymmetric order of high dipole moment high hyperpolarizability chromophores in electrically poled polymeric thin films. *Proc. Natl. Acad. Sci. U. S. A.* **1997**, *94*, 4842–4847.

(55) Dalton, L. R.; Steier, W. H.; Robinson, B. H.; Zhang, C.; Ren, A.; Garner, S.; Chen, A. T.; Londergan, T.; Irwin, L.; Carlson, B.; Fifield, L.; Phelan, G.; Kincaid, C.; Amend, J.; Jen, A. From molecules to opto-chips: organic electro-optic materials. *J. Mater. Chem.* **1999**, *9*, 1905–1920.

(56) Liakatas, I.; Cai, C.; Bösch, M.; Jäger, M.; Bosshard, C.; Günter, P.; Zhang, C.; Dalton, L. R. Importance of intermolecular interactions in the nonlinear optical properties of poled polymers. *Appl. Phys. Lett.* **2000**, *76*, 1368–1370.

(57) Luo, J.; Haller, M.; Ma, H.; Liu, S.; Kim, T.-D.; Tian, Y.; Chen, B.; Jang, S.-H.; Dalton, L. R.; Jen, A. K.-Y. Nanoscale architectural control and macromolecular engineering of nonlinear optical dendrimers and polymers for electro-optics. *J. Phys. Chem. B* **2004**, *108*, 8523–8530.

(58) Robinson, B. H.; Dalton, L. R.; Harper, A. W.; Ren, A.; Wang, F.; Zhang, C.; Todorova, G.; Lee, M.; Aniszfeld, R.; Garner, S.; Chen, A.; Steier, W. H.; Houbrecht, S.; Persoons, A.; Ledoux, I.; Zyss, J.; Jen, A. K.-Y. The molecular and supramolecular engineering of polymeric electro-optic materials. *Chem. Phys.* **1999**, *245*, 35–50.

(59) Steier, W. H.; Chen, A.; Lee, S.-S.; Garner, S.; Zhang, H.; Chuyanov, V.; Dalton, L. R.; Wang, F.; Ren, A. S.; Zhang, C.; Todorova, G.; Harper, A.; Fetterman, H. R.; Chen, D.; Udupa, A.; Bhattacharya, D.; Tsap, B. Polymer electro-optic devices for integrated optics. *Chem. Phys.* **1999**, *245*, 487–506.

(60) Brédas, J. L.; Meyers, F.; Pierce, B. M.; Zyss, J. On the second-order polarizability of conjugated p-electron molecules with octupolar symmetry: the case of triaminotrinitrobenzene. *J. Am. Chem. Soc.* **1992**, *114*, 4928–4929.

(61) Cho, B. R.; Park, S. B.; Lee, S. J.; Son, K. H.; Lee, S. H.; Lee, M.-J.; Yoo, J.; Lee, Y. K.; Lee, G. J.; Kang, T. I.; Cho, M.; Jeon, S.-J. 1,3,5-tricyano-2,4,6-tris(vinyl)benzene derivatives with large second-order nonlinear optical properties. *J. Am. Chem. Soc.* **2001**, *123*, 6421–6422.

(62) Hennrich, G.; Asselberghs, I.; Clays, K.; Persoons, A. Tuning octopolar nlo chromophores: synthesis and spectroscopic character-ization of persubstituted 1,3,5-tris(ethynylphenyl)benzenes. *J. Org. Chem.* **2004**, *69*, 5077–5081.

(63) Hennrich, G.; Omenat, A.; Asselberghs, I.; Foerier, S.; Clays, K.; Verbiest, T.; Serrano, J. L. Liquid crystals from C_3-symmetric mesogens for second-order nonlinear optics. *Angew. Chem., Int. Ed.* **2006**, *45*, 4203–4206.

(64) Kim, H. M.; Cho, B. R. Second-order nonlinear optical properties of octupolar molecules structure-property relationship. *J. Mater. Chem.* **2009**, *19*, 7402–7409.

(65) Lambert, C.; Nöll, G.; Schmälzlin, E.; Meerholz, K.; Bräuchle, C. Synthesis, (non)linear optical and redox properties of a donor-substituted truxenone derivative. *Chem. - Eur. J.* **1998**, *4*, 2129–2135.

(66) Le Bozec, H.; Le Bouder, T.; Maury, O.; Bondon, A.; Ledoux, I.; Deveau, S.; Zyss, J. Supramolecular octupolar self-ordering towards nonlinear optics. *Adv. Mater.* **2001**, *13*, 1677–1681.

(67) Le Floc'h, V.; Brasselet, S.; Zyss, J.; Cho, B. R.; Lee, S. H.; Jeon, S.-J.; Cho, M.; Min, K. S.; Suh, M. P. High efficiency and quadratic nonlinear optical properties of a fully optimized 2D octupolar crystal characterized by nonlinear microscopy. *Adv. Mater.* **2005**, *17*, 196–200.

(68) Maury, O.; Le Bozec, H. Molecular engineering of octupolar NLO molecules and materials based on bipyridyl metal complexes. *Acc. Chem. Res.* **2005**, *38*, 691–704.

(69) McDonagh, A. M.; Humphrey, M. G.; Samoc, M.; Luther-Davies, B.; Houbrechts, S.; Wada, T.; Sasabe, H.; Persoons, A. Organometallic complexes for nonlinear optics. 16. Second and third

order optical nonlinearities of octopolar alkynylruthenium complexes. *J. Am. Chem. Soc.* **1999**, *121*, 1405−1406.

(70) Verbiest, T.; Clays, K.; Samyn, C.; Wolff, J.; Reinhoudt, D.; Persoons, A. Investigations of the hyperpolarizability in organic molecules from dipolar to octopolar systems. *J. Am. Chem. Soc.* **1994**, *116*, 9320−9323.

(71) Wolff, J. J.; Siegler, F.; Matschiner, R.; Wortmann, R. Optimized two-dimensional NLO chromophores with a threefold symmetry axis. *Angew. Chem., Int. Ed.* **2000**, *39*, 1436−1439.

(72) Zyss, J.; Dhenaut, C.; Chauvan, T.; Ledoux, I. Quadratic nonlinear susceptibility of octupolar chiral ions. *Chem. Phys. Lett.* **1993**, *206*, 409−414.

(73) Ostroverkhov, V.; Singer, K. D.; Petschek, R. G. Second-harmonic generation in nonpolar chiral materials: relationship between molecular and macroscopic properties. *J. Opt. Soc. Am. B* **2001**, *18*, 1858−1865.

(74) Bartholomew, G. P.; Ledoux, I.; Mukamel, S.; Bazan, G. C.; Zyss, J. Three-dimensional nonlinear optical chromophores based on through-space delocalization. *J. Am. Chem. Soc.* **2002**, *124*, 13480−13485.

(75) Tai, O. Y.-H.; Wang, C. H.; Ma, H.; Jen, A. K.-Y. Wavelength dependence of first molecular hyperpolarizability of a dendrimer in solution. *J. Chem. Phys.* **2004**, *121*, 6086−6092.

(76) Stadler, S.; Dietrich, R.; Bourhill, G.; Bräuchle, C.; Pawlik, A.; Grahn, W. First hyperpolarizability measurements via hyper-Rayleigh scattering at 1500 nm. *Chem. Phys. Lett.* **1995**, *247*, 271−276.

(77) Stadler, S.; Dietrich, R.; Bourhill, G.; Bräuchle, C. Long-wavelength first hyperpolarizability measurements by hyper-Rayleigh scattering. *Opt. Lett.* **1996**, *21*, 251−253.

(78) Schmälzlin, E.; Meerholz, K.; Stadler, S.; Bräuchle, C.; Patzelt, H.; Oesterhelt, D. Molecular first hyperpolarizabilities of retinal and its derivatives. *Chem. Phys. Lett.* **1997**, *280*, 551−555.

(79) Büchert, M.; Steenbock, T.; Lukaschek, C.; Wolff, M. C.; Herrmann, C.; Heck, J. 2,2′-bipyridine-based dendritic structured compounds for second harmonic generation. *Chem. - Eur. J.* **2014**, *20*, 14351−14361.

(80) Silva, T. J. L.; Mendes, P. J.; Garcia, M. H.; Robalo, M. P.; Ramalho, J. P. P.; Carvalho, A. J. P.; Büchert, M.; Wittenburg, C.; Heck, J. Benzo[c]thiophene chromophores linked to cationic fe and ru derivatives for NLO materials: synthesis characterization and quadratic hyperpolarizabilities. *Eur. J. Inorg. Chem.* **2013**, *2013*, 3506−3517.

(81) Silva, T. J. L.; Mendes, P. J.; Santos, A. M.; Garcia, M. H.; Robalo, M. P.; Ramalho, J. P. P.; Carvalho, A. J. P.; Büchert, M.; Wittenburg, C.; Heck, J. Mono(η_5-cyclopentadienyl)metal(II) complexes with thienyl acetylide chromophores: synthesis, electrochemical studies, and first hyperpolarizabilities. *Organometallics* **2014**, *33*, 4655−4671.

(82) DiMagno, S. G.; Lin, V. S.-Y.; Therien, M. J. Facile elaboration of porphyrins via metal-mediated cross-coupling. *J. Org. Chem.* **1993**, *58*, 5983−5993.

(83) DiMagno, S. G.; Lin, V. S.-Y.; Therien, M. J. Catalytic conversion of simple haloporphyrins into alkyl-, aryl-, pyridyl-, and vinyl-substituted porphyrins. *J. Am. Chem. Soc.* **1993**, *115*, 2513−2515.

(84) Heck, R. F. Palladium-catalyzed reactions of organic halides with olefins. *Acc. Chem. Res.* **1979**, *12*, 146−151.

(85) Kumada, M. Nickel and palladium complex catalyzed cross-coupling reactions of organometallic reagents with organic halides. *Pure Appl. Chem.* **1980**, *52*, 669−679.

(86) Negishi, E.; Luo, F. T.; Frisbee, R.; Matsushita, H. Selective carbon-carbon bond formation via transition metal catalysis. 26. A regiospecific synthesis of carbo-substituted heteroaromatic derivatives via palladium-catalyzed cross coupling. *Heterocycles* **1982**, *18*, 117−122.

(87) Stille, J. K. Palladium-catalyzed coupling reactions of organic electrophiles with organic tin compounds. *Angew. Chem., Int. Ed. Engl.* **1986**, *25*, 508−524.

(88) Takahashi, S.; Kuroyama, Y.; Sonogashira, K.; Hagihara, N. A convenient synthesis of ethynylarenes and diethynylarenes. *Synthesis* **1980**, *1980*, 627−630.

(89) Ishizuka, T.; Sinks, L. E.; Song, K.; Hung, S.-T.; Nayak, A.; Clays, K.; Therien, M. J. The roles of molecular structure and effective optical symmetry in evolving dipolar chromophoric building blocks to potent octopolar nonlinear optical chromophores. *J. Am. Chem. Soc.* **2011**, *133*, 2884−2896.

(90) DiMagno, S. G.; Williams, R. A.; Therien, M. J. Facile synthesis of meso-tetrakis(perfluoroalkyl)porphyrins: spectroscopic properties and x-ray crystal structure of highly electron-deficient 5,10,15,20-tetrakis(heptafluoropropyl)porphyrin. *J. Org. Chem.* **1994**, *59*, 6943−6948.

(91) Goll, J. G.; Moore, K. T.; Ghosh, A.; Therien, M. J. Synthesis, structure, electronic spectroscopy, photophysics, electrochemistry, and x-ray photoelectron spectroscopy of highly-electron-deficient [5,10,15,20-tetrakis(perfluoroalkyl)porphinato]zinc(II) complexes and their free base derivatives. *J. Am. Chem. Soc.* **1996**, *118*, 8344−8354.

(92) Moore, K. T.; Fletcher, J. T.; Therien, M. J. Syntheses, NMR and EPR spectroscopy, electrochemical properties, and structural studies of [5,10,15,20-tetrakis(perfluoroalkyl)porphinato]iron(II) and -iron(III) complexes. *J. Am. Chem. Soc.* **1999**, *121*, 5196−5209.

(93) Notaras, E. G. A.; Fazekas, M.; Doyle, J. J.; Blau, W. J.; Senge, M. O. A₂B₂-type push−pull porphyrins as reverse saturable and saturable absorbers. *Chem. Commun.* **2007**, *43*, 2166−2168.

(94) LeCours, S. M.; Philips, C. M.; de Paula, J. C.; Therien, M. J. Synthesis, transient absorption, and transient resonance Raman spectroscopy of novel electron donor-acceptor complexes: [5,15-bis[(4 ′-nitrophenyl)ethynyl]-10,20-diphenylporphinato]copper(II) and [5-[[4 ′-(dimethylamino)phenyl]ethynyl]-15-[(4 ″-nitrophenyl)-ethynyl]-10,20-diphenyl-porphinato]copper(II). *J. Am. Chem. Soc.* **1997**, *119*, 12578−12589.

(95) Uyeda, H. T. PhD Thesis; University of Pennsylvania: 2002.

(96) Damrauer, N. H.; Boussie, T. R.; Devenney, M.; McCusker, J. K. Effects of intraligand electron delocalization, steric tuning, and excited-state vibronic coupling on the photophysics of aryl-substituted bipyridyl complexes of Ru(II). *J. Am. Chem. Soc.* **1997**, *119*, 8253−8268.

(97) Damrauer, N. H.; Weldon, B. T.; McCusker, J. K. Theoretical studies of steric effects on intraligand electron delocalization: implications for the Franck-Condon state evolution of MLCT excited states. *J. Phys. Chem. A* **1998**, *102*, 3382−3397.

(98) McCusker, J. K. Femtosecond absorption spectroscopy of transition metal charge-transfer complexes. *Acc. Chem. Res.* **2003**, *36*, 876−887.

(99) Winkler, J. R.; Netzel, T. L.; Creutz, C.; Sutin, N. Direct observation of metal-to-ligand charge-transfer (MLCT) excited states of pentaammineruthenium(II) complexes. *J. Am. Chem. Soc.* **1987**, *109*, 2381−2392.

(100) Kumble, R.; Palese, S.; Lin, V. S.-Y.; Therien, M. J.; Hochstrasser, R. M. Ultrafast dynamics of highly conjugated porphyrin arrays. *J. Am. Chem. Soc.* **1998**, *120*, 11489−11498.

(101) Oudar, J. L. Optical nonlinearities of conjugated molecules. Stilbene derivatives and highly polar aromatic compounds. *J. Chem. Phys.* **1977**, *67*, 446−457.

(102) Oudar, J. L.; Chemla, D. S. Hyperpolarizabilities of nitroanilines and their relations to excited state dipole moment. *J. Chem. Phys.* **1977**, *66*, 2664−2668.

(103) Cyvin, S. J.; Rauch, J. E.; Decius, J. C. Theory of hyper-raman effects (nonlinear inelastic light scattering) - selection rules and depolarization ratios for second-order polarizability. *J. Chem. Phys.* **1965**, *43*, 4083−4094.

(104) Bersohn, R.; Pao, Y.-H.; Frisch, H. L. Double-quantum light scattering by molecules. *J. Chem. Phys.* **1966**, *45*, 3184−3198.

(105) Champagne, B.; Pèrpete, E. A.; van Gisbergen, S. J. A.; Baerends, E.-J.; Snijders, J. G.; Soubra-Ghaoui, C.; Robins, K. A.; Kirtman, B. Assessment of conventional density functional schemes for computing the polarizabilities and hyperpolarizabilities of conjugated oligomers: An ab initio investigation of polyacetylene chains. *J. Chem. Phys.* **1998**, *109*, 10489−10498.

(106) Jamorski, C.; Casida, M. E.; Salahub, D. R. Dynamic polarizabilities and excitation spectra from a molecular implementation of time-dependent density-functional response theory: N_2 as a case study. *J. Chem. Phys.* **1996**, *104*, 5134−5147.

(107) Karna, S. P.; Prasad, P. N.; Dupuis, M. Nonlinear optical properties of p-nitroaniline: an ab initio time-dependent coupled perturbed hartree-fock study. *J. Chem. Phys.* **1991**, *94*, 1171−1181.

(108) Kirtman, B.; Champagne, B. Nonlinear optical properties of quasilinear conjugated oligomers, polymers and organic molecules. *Int. Rev. Phys. Chem.* **1997**, *16*, 389−420.

(109) Tretiak, S.; Chernyak, V. Resonant nonlinear polarizabilities in the time-dependent density functional theory. *J. Chem. Phys.* **2003**, *119*, 8809−8823.

(110) Tretiak, S.; Mukamel, S. Density matrix analysis and simulation of electronic excitations in conjugated and aggregated molecules. *Chem. Rev.* **2002**, *102*, 3171−3212.

(111) van Gisbergen, S. J. A.; Kootstra, F.; Schipper, P. R. T.; Gritsenko, O. V.; Snijders, J. G.; Baerends, E. J. Density-functional-theory response-property calculations with accurate exchange-correlation potentials. *Phys. Rev. A: At., Mol., Opt. Phys.* **1998**, *57*, 2556−2571.

(112) van Gisbergen, S. J. A.; Snijders, J. G.; Baerends, E. J. Calculating frequency-dependent hyperpolarizabilities using time-dependent density functional theory. *J. Chem. Phys.* **1998**, *109*, 10644−10656.

(113) Champagne, B.; Pèrpete, E. A.; Jacquemin, D.; van Gisbergen, S. J. A.; Baerends, E.-J.; Soubra-Ghaoui, C.; Robins, K. A.; Kirtman, B. Assessment of conventional density functional schemes for computing the dipole moment and (hyper)polarizabilities of push-pull π-conjugated systems. *J. Phys. Chem. A* **2000**, *104*, 4755−4763.

(114) Miura, M.; Aoki, Y.; Champagne, B. Assessment of time-dependent density functional schemes for computing the oscillator strengths of benzene, phenol, aniline, and fluorobenzene. *J. Chem. Phys.* **2007**, *127*, 084103.

(115) Kelley, A. M. Frequency-dependent first hyperpolarizabilities from linear absorption spectra. *J. Opt. Soc. Am. B* **2002**, *19*, 1890−1900.

(116) Olivier, J.-H.; Bai, Y.; Uh, H.; Yoo, H.; Therien, M. J.; Castellano, F. N. Near infrared-to-visible photon upconversion enabled by conjugated porphyrinic sensitizers under low-power noncoherent illumination. *J. Phys. Chem. A* **2015**, *119*, 5642−5649.

(117) Olbrechts, G.; Strobbe, R.; Clays, K.; Persoons, A. High-frequency demodulation of multi-photon fluorescence in hyper-Rayleigh scattering. *Rev. Sci. Instrum.* **1998**, *69*, 2233−2241.

(118) Olbrechts, G.; Wostyn, K.; Clays, K.; Persoons, A. High-frequency demodulation of multiphoton fluorescence in long-wave-length hyper-Rayleigh scattering. *Opt. Lett.* **1999**, *24*, 403−405.

(119) Campo, J.; Painelli, A.; Terenziani, F.; Van Regemorter, T.; Beljonne, D.; Goovaerts, E.; Wenseleers, W. First hyperpolarizability dispersion of the octupolar molecule crystal violet: multiple resonances and vibrational and solvation effects. *J. Am. Chem. Soc.* **2010**, *132*, 16467−16478.

(120) Woodford, J. N.; Pauley, M. A.; Wang, C. H. Solvent dependence of the first molecular hyperpolarizability of p-nitroaniline revisited. *J. Phys. Chem. A* **1997**, *101*, 1989−1992.

(121) Van Cleuvenbergen, S.; Asselberghs, I.; García-Frutos, E. M.; Gómez-Lor, B.; Clays, K.; Pérez-Moreno, J. Dispersion overwhelms charge transfer in determining the magnitude of the first hyper-polarizability in triindole octupoles. *J. Phys. Chem. C* **2012**, *116*, 12312−12321.